Microsyst Technol (2015) 21:117–122
DOI 10.1007/s00542-013-1937-2

TECHNICAL PAPER

Graphene diaphragm analysis for pressure or acoustic sensor applications

Dongxue Wang · Shangchun Fan · Wei Jin

Received: 23 August 2013 / Accepted: 2 October 2013 / Published online: 19 October 2013

Abstract Graphene has remarkable mechanical properties, and it is a very promising material for sensors. The progress of graphene diaphragm based pressure sensor was detailed firstly. Then the deflection of pressurized circular graphene diaphragm with pre-stress was discussed, an approximate solution was given to substitute Hencky's series solution. Pre-stress descends the sensitivity of the graphene diaphragm, but it also makes the deflection linear in pre-stress dominated regime, which is important for sensor applications. The pre-stress in the diaphragm caused by van der Waals force between the diaphragm and the sidewall of the substrate was studied, the results indicates that the pre-stress is associated with the adhesion energy per unit area between the diaphragm and sidewall of the substrates, and the thickness of the diaphragm. Due to the influence of the the adhesion force, multilayer (2 ~ 10 layers) graphene diaphragms are more sensitive than monolayer, as monolayer graphene is much more flexible, the adhesion energy is higher than multilayer graphene.

Abbreviations

p	Applied pressure
h	Center deflection of the membrane
a	Radius of the diaphragm
t	Thickness of the diaphragm
v	Poisson ratio
E	Young's modulus
ε_r	Radial strains
ε_r	Circumferential strains
N_r	Forces per unit length in radial direction
N_t	Forces per unit length in circumferential direction
σ_0	Pre-stress in the diaphragm
σ_r	Stress in the radial direction
σ_t	Stress in the circumferential direction
Γ	Adhesion energy per unit area

D. Wang (✉) · S. Fan
School of Instrument Science and Opto-electronics Engineering, Beihang University, Beijing 100191, China
e-mail: wdongxue18@163.com

D. Wang · S. Fan
Science and Technology on Inertial Laboratory, Beihang University, Beijing 100191, China

W. Jin
Department of Electrical Engineering, The Hong Kong Polytechnic University, Hung Hom, Kowloon, China

1 Introduction

Graphene consists of a single layer or multi layers of carbon atoms bonded by strong covalent bonds within a layer but weaker van der Waals bonds between layers. The thickness of monolayer graphene is ~0.335 nm, which is the thinnest material ever find in the world. Graphene has remarkable mechanical and electrical properties (Geim 2009), these properties make graphene a very promising material for electronic devices and sensors (Lin et al. 2010; Bunch et al. 2007; Ma et al. 2012; El-Kady et al. 2012). The mechanical properties of graphene include a high in-plane Young's modulus of ~1TPa probed using nano-indentation of suspended graphene (Lee et al. 2008), force extension measurements (Gómez-Navarro et al. 2008) and electromechanical resonators (Chen et al. 2009; Garcia-Sanchez et al. 2008) The breaking strength of a defect-free sheet is 42 N m^{-1} (Lee et al. 2008), correspond to an intrinsic strength of $\sigma_{int} = 130$ GPa, which is 100 times greater than steel (250–1,200 MPa). Graphene is flexible and can be

stretched by as much as 20 percent without inducing defects (Kim et al. 2009).

Bunch et al. (2008) reported that the mechanical exfoliated graphene membrane is impermeable to standard gases including helium, the study suggests that graphene may be used for pressure sensors. Graphene based diaphragms are quite sensitive to the subjected pressures due to their ultra-thin properties.

Graphene sheets clamp to substrates by van der Waals force which are much weaker than cowalent bonds. Graphene diaphragms may be deboned from the substrates by applied pressure. Koenig et al. (2011) use a pressurized bister test demonstrated that suspended graphene has much higher mechanical strength than silica and could withstand a static pressure up to 2.5 MPa with SiO_2 substrate.

Smith et al. (2012) reported that pressure-induced band structure changes on strained graphene membrane could be detected electrically, suggesting the application as ultra-sensitive MEMS or NEMS pressure sensors. Ma et al. (2012) built a miniature fiber-tip Fabry–Perot pressure sensor by using an extremely thin graphene diaphragm. The graphene based sensor demonstrated pressure sensitivity over 39.4 nm/kPa with a diaphragm diameter of 25 μm, the sensitivity is higher than any other pressure sensors with the same size. Later they fabricated a fiber-optic Fabry–Perot acoustic sensor with a $\sim$100 nm-thick graphene diaphragm. The sensor demonstrates a pressure induced deflection of 1,100 nm/kPa, which is the highest being reported so far to our knowledge (Ma et al. 2013).

Fiber-tip Fabry–Perot Interferometric (FPI) may detect displacements less than several pm, and have the advantages of good temperature stability, immunity to electromagnetic interference. They are suited for graphene based sensors. Figure 1 is the schematic of a sensor head that comprises of a ferrule, a standard single mode fiber (SMF), and a graphene diaphragm adheres to the ferrule by strong Van der Waals force. The interspace between the fiber end and the graphene diaphragm forms a sealed chamber. The reflective surfaces at the cleaved fiber end and the graphene diaphragm form a low-finesse FPI, and the deflection of the diaphragm can be determined by detecting the intensity or spectrum of the reflected light.

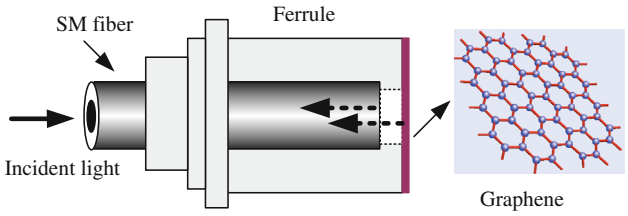

Fig. 1 Schematic of a typical fiber-optic FPI sensor with graphene diaphragm

However, the mechanical behaviors of graphene diaphragms are strongly influenced by van der Waals force with substrates, and the influence to graphene diaphragm is not clear. Numerous researchers report that suspended graphene membrane is in a strong self-tensioning. The pre-stress of monolayer graphene suspended on SiO_2 with circular cavity is measured by using of an AFM tip method (Lee et al. 2008), the values varied from 0.2 to 2.2 GPa. Ma et al. (2012) measured the pre-stress of suspended graphene and from the research we find that the pre-stress decreased with the thickness. The amount of pre-stress is partly dependent on the strong van der Waals interaction between the edge of the graphene membrane and the substrates sidewalls.

In this paper, we studied the deflections of clamped circular graphene diaphragm under uniform pressure firstly, including small deflection (linear deflection model) of thick graphene film and large deflections with pre-stress inner the membrane. Then we analyzed the pre-stress caused by adhesion force between membrane and side wall of the substrate in Sect. 3. The sensitivity and linearity of graphene diaphragm was discussed in Sect. 4.

2 Deflections under uniform pressure

The diaphragm here is axisymmetric structure clamped at a radial position. The radial boundary is located at $r = a$. The thickness of graphene diaphragm varies from 0.335 nm to several hundred nanometers. There are two different models to describe the mechanical behavior of the circular diaphragm: one is thick membrane with small deflections and thin membrane with large deflections.

2.1 Small deflections of graphene film

For thick diaphragms with deflections no more than $20\sim30$ % of the diaphragm thickness, the center deflection of the round film is a function of the pressure given by (Di Giovanni 1982)

$$h = \frac{3(1-v^2)a^4}{16Et^3}p. \tag{1}$$

Here $v = 0.17$, $E = 1$TPa for graphene (Ma et al. 2012).

2.2 Large deflections of graphene membrane

While the center deflection is large compares to the thickness of the diaphragm, the mechanical behavior of the diaphragm can be described by Foppl-von Karman (FvK) equations. Hencky (1915) obtained a series solution of the FvK equations with bending rigidity being neglected

$$p = k_v \times \frac{Et}{a^4} h^3. \tag{2}$$

Here, k_v is a constant dependent on the Poisson's ratio, we use $k_v = 3.12$ for $v = 0.17$ ($k_v = 3.09$ for $v = 0.16$). Hencky's solution is formally for the case of a uniformly distributed load on the diaphragm, which simplifies the analysis and can be used for deflections much smaller compares to the radius of the diaphragm. However, the deflection is nonlinear against the pressure, which is not convenient for data acquisition and processing.

Hencky's solution does not consider the effect of the initial stress in the diaphragm. Campbell and Vlassak extended Hencky's solution to cases with an initial stress σ_0. In initial stress dominated regime that

$$\frac{4(1-v)\sigma_0}{E}\left(\frac{Et}{pa}\right)^{\frac{2}{3}} \gg 1. \tag{3}$$

The relation of pressure p and the center deflection h may be written as (Campbell 1956; Vlassak 1994)

$$p = 4 \times \frac{\sigma_0 t}{a^2} h. \tag{4}$$

The relationship of Eq. (4) is linear, and this may be very useful for graphene based sensor applications. For small initial stress or large applied pressure such that

$$\frac{pa}{Et} > 100\left(\frac{\sigma}{E}\right)^{\frac{3}{2}}. \tag{5}$$

The deflection given by Eq. (2) is within 5 % of the solution with σ_0 taken into account.

A rough solution to the general case can be obtained by superposing the solutions of two limiting cases. Given by

$$p = k_v \times \frac{Et}{a^4} h^3 + 4 \times \frac{\sigma_0 t}{a^2} h. \tag{6}$$

The equation was proved accurate enough to substitute Hencky's series solution by Vlassak. The function here is similar with the solution given by Beams (1959) and Lin (1990), only the coefficient k_v of the three functions are slightly different.

In order to assess the accuracy of the approximate solution Eq. (6) further, finite element method (FEM) is introduced for the simulation of pressure-deflection behavior of suspended graphene membrane. FEM is believed more accurate than analytic solutions due to more accurate deflected shapes predicted by simulations.

The model here is meshed with 2-node axisymmetric shell element with three degrees of freedom at each node. The element allows us to account for large strain effects and layers in our model. With the powerful computing capabilities of ANSYS, we can get the stress, strain, and the displacement values of every node. Figure 2 shows the center displacement of different membranes plotted against the pressure, indicates that the results by FEM simulation are extremely close to our approximate solution when the deflection of the membrane is small compares to the radius of the membrane ($h/a < 20$ %).

3 Initial stress caused by adhesion force

For circular graphene membrane with no residual stress due to processing at the initial state. Van der Waals force causes the membrane to laminate onto the substrate and wrap down the sidewall of the cavity (shown as Fig. 3). The force stretches the membrane and causing tension which is process independent. Both of the adhesion forces and strains in the membrane are axisymmetric.

Assume the membrane is adhered to the sidewall over a length u_0 at the equilibrium position. The non-dimensional boundary condition is $u(0) = 0$ and $u(a) = u_0$. There is only radial stretching displacement in the plane of the membrane. $dw/dr = 0$ due to the membrane is flat.

For annular membranes with inner radius b and out radius a, the radial displacement may be written as (Géminard et al. 2004)

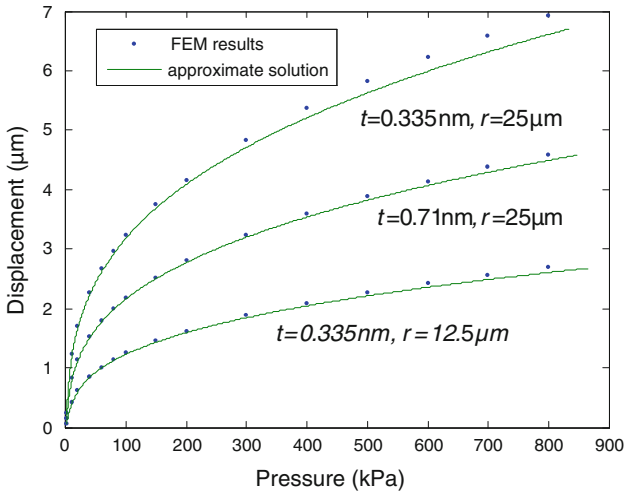

Fig. 2 Center displacement of circular graphene diaphragm derived by the approximate solution and finite element simulation

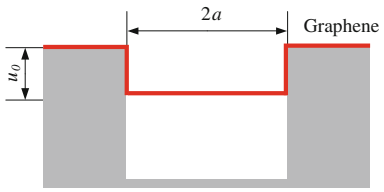

Fig. 3 Schematic of the graphene membrane on the substrate with circular cavity, the membrane laminate onto the substrate and wrap down the sidewall of the cavity

$$u(r) = \frac{u_0}{a}\left(r^2 - b^2\right) \Big/ \left[r(1-b^2)\right]. \tag{7}$$

As the discussed circular membrane here with $b = 0$, the displacement in radius direction can be obtained $u(a) = u_0 \cdot r/a$. The radial and circumferential strains is

$$\varepsilon_r = \varepsilon_t = \frac{u_0}{a}. \tag{8}$$

The tension in the radial and circumferential direction can be expressed as

$$N_r = N_t = \frac{Et}{1-v}\frac{u_0}{a} \tag{9}$$

The stress caused by surface force between the membrane and side wall is called pre-stress here. Let σ_0 be the pre-stress, Γ be the adhesion energy per unit area between the edge of the membrane and the side wall of the substrates. The elastic strain energy V_{strain} due to stretching can be obtained

$$V_{strain} = \frac{1}{2}\int_A (N_r\varepsilon_r + N_t\varepsilon_t) r dr d\theta. \tag{10}$$

Substituting Eqs. (8) and (9) to Eq. (10), then integration yields

$$V_{strain} = \pi a t \sigma_0 u_0. \tag{11}$$

The adhesion energy V_{van} may be written as Eq. (12) approximately

$$V_{van} = 2\pi a u_0 \Gamma. \tag{12}$$

The bending energy can be neglected here due to graphene is flexible. The total potential energy of the deformed system is $V = V_{strain} - V_{van}$. Minimizing the potential energy yields the equilibrium stress σ_0

$$\sigma_0 = \frac{2}{t}\Gamma. \tag{13}$$

The pre-stress σ_0 is associated with the adhesion energy per unit area and the thickness of the membrane.

4 Sensitivity analysis

By Eq. (6) we find that the sensitivity of the diaphragm may be reduced as the thickness increases for most cases. But Eq. (6) is a nonlinear equation which is difficult for data processing. For the convenient of data acquisition and processing, most of the applications for pressure and acoustic sensors require the deflection of the membrane against pressure is linear. From the analysis above, the deflection is linear against the pressure when Eq. (3) is satisfied.

Equation (4) may be rewritten as

$$h = \frac{1}{4} \times \frac{a^2}{\sigma_0 t} p \tag{14}$$

The deflection of the pressurized membrane is nonlinear without pre-stress. On the other hand the pre-stress may descend the sensitivity of the membrane if it is too large. So the pre-stress must be considered in the design of pressure sensor or acoustic sensor.

From the analysis above, the pre-stress may be influenced by the adhesion energy per unit area. In pre-stress dominated regime, the deflection of the diaphragm can be obtained by substituting Eq. (13) to Eq. (4),

$$h = \frac{1}{8} \times \frac{a^2}{\Gamma} p. \tag{15}$$

By Eqs. (3) and (13), the pre-stress dominated regime may be written as

$$p \ll 16 \times \left(\frac{(1-v)^3\Gamma^3}{Eta^2}\right)^{1/2}. \tag{16}$$

The deflection associated with adhesion energy Γ and has no relation with the thickness of the diaphragm. Γ may decrease the sensitivity of the diaphragm, but a larger Γ also increases the range of linear deflections.

Various experimental methods have been taken to determine the adhesion energy between graphene and different substrates. Yoon et al. (2012) directly measured the adhesion energy of CVD grown graphene on copper, adhesion energies of 0.72 J m^{-2} were found. Koenig et al. (2011) find adhesion energy of 0.45 + 0.02 J m^{-2} for monolayer graphene with a silicon oxide substrate and 0.31 + 0.03 J m^{-2} for samples containing two to five graphene sheets. The adhesion energies of multilayer graphene with silicon oxide substrate are lower than monolayer, they infer that this may due to monolayer graphene is more flexible and can conform to the topography of even the smoothest substrates, thus making its interaction with the substrate more liquid-like than solid-like. Recently their new measurements show a lower average value of 0.24 J m^{-2} for monolayer graphene (Boddeti et al. 2013), they deduce that the adhesion energy differences of the two measurements could arise from differences in surface properties, such as roughness and chemical reactivity, and thus change the apparent adhesion energy.

The pre-stress may be determined by selecting different substrate due to Γ is varies for different materials. Furthermore, Gao and Huang (2011) reported that the surface roughness may affect the adhesion between graphene membranes and their substrates, suggest that tunable adhesion can be achieved by controlling the surface roughness of the substrate. The research indicates that the values of adhesion energy are approximately the same.

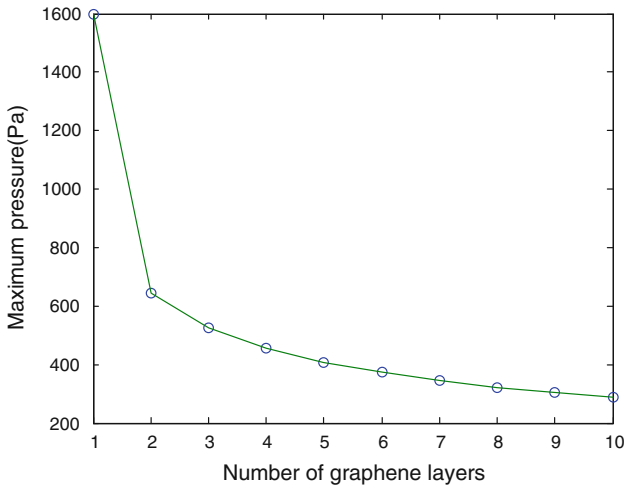

Fig. 4 The maximum pressure as a function of the number of graphene layers ($r = 12.5$ μm), the deflection is linear under the maximum pressure

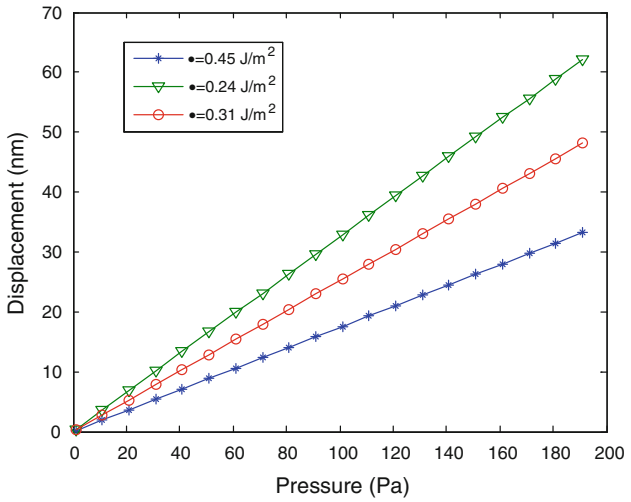

Fig. 5 Center deflection of circular graphene with different adhesion energies versus applied pressure in pre-stress dominated regime

Let p_{max} be the maximum pressure to keep the model in pre-stress dominated regime and p_{max} equals to the r.h.s. of Eq. (16) divide by ten,

$$p_{\max} = 1.6 \times \left(\frac{(1-v)^3 \Gamma^3}{Eta^2} \right)^{1/2}. \tag{17}$$

We assume that silicon oxide is used as the substrate of the sensor, and the adhesion energy is 0.45 J m^{-2} for monolayer graphene with the substrate and 0.31 J m^{-2} for two to ten layers graphene sheets. For graphene diaphragm with diameters of 25 μm, p_{max} derived by Eq. (17) is shown as Fig. 4.

The values of p_{max} reduce as the number of layers increases. The maximum value of p_{max} is no more than 1,600 kPa. The result demonstrates that graphene

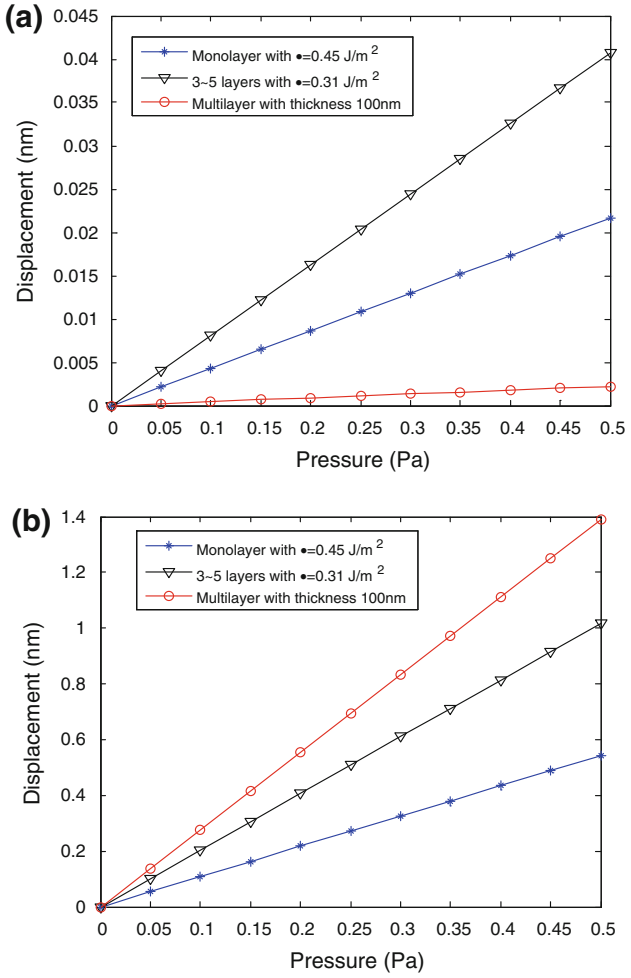

Fig. 6 Center deflection of circular graphene with different, radius versus applied pressure **a** radius $r = 12.5$ μm **b** radius, $r = 62.5$ μm

diaphragm may be used as acoustic sensors and ultra-low pressure sensors. The curve of center displacements against applied pressures is shown as Fig. 5. The sensitivity of 2 ~ 10 layers graphene is ~250 nm/kPa, more than 170 nm/kPa for monolayer.

For graphene diaphragm with thickness $t = 100$ nm and radius of 12.5 and 62.5 μm respectively, assume the center deflection is no more than 30 nm, the center-displacements against applied pressures is shown as Fig. 6a ($r = 12.5$ μm) and Fig. 6b ($r = 62.5$ μm). In order to compare the sensitivity against applied pressures, the deflections of monolayer and 2 ~ 5 layers are also included. From Fig. 6a, we can find that monolayer or 2 ~ 5 layers graphene are much more sensitive than graphene diaphragm with $t = 100$ nm in linear model, but they are less sensitive than the thick diaphragm at Fig. 6b, as the sensitivity of linear deflection model increases more quickly as diameters become larger. The results suggest that the ultra-thin graphene diaphragms have prospects to be used as ultra-small pressure of acoustic sensors.

From the research above, we find it is interesting that multilayer (2∼5 layers) may be more sensitive than monolayer graphene due to the higher pre-stress of monolayer graphene.

5 Conclusions

For thin multilayer graphene diaphragm without pre-stress, if the deflection is smaller than 30 % of the thickness of the diaphragm, which called small deflections, the linear model is applicable as Eq. (1). For large deflections, they are also linear as described in Eq. (4) in pre-stress dominated regime. The two linear models are quite useful for sensor applications.

We studied the stress in the graphene diaphragm caused by strong van der Waals force between the diaphragm and the side wall of the substrate. The stress of the diaphragm cannot be eliminated and has relation with the thickness of the diaphragm and the adhesion energy per unit area between the diaphragm and side wall of the substrates. The adhesion of Graphene and substrate is strong compared to typical micro- mechanical structures and may influence the performance of the sensor.

We find the adhesion descends the sensitivity of the diaphragm in pre-stress dominated regime. The sensitivity of multilayer graphene diaphragm is higher than monolayer due to the adhesion force. We can adjust the adhesion energy to improve the sensitivity of the diaphragm by controlling the surface roughness of the substrates or selecting different materials. Graphene diaphragms are very sensitive to subjected pressures, and they would find applications in miniature, highly sensitive pressure and acoustic sensors.

Acknowledgments This work is supported by Program for Changjiang Scholars and Innovative Research Team in University (PCSIRT), the National Nature Science Fund of china with grant No. 61273060 and 61121003.

References

Beams JW (1959) Mechanical properties of thin films of gold and silver. Structure and properties of thin films pp 183–192

Boddeti NG, Koenig SP, Long R et al (2013) Mechanics of adhered, pressurized graphene blisters. J Appl Mech 80:040909. doi:10.1115/1.4024255

Bunch JS, Van Der Zande AM, Verbridge SS et al (2007) Electromechanical resonators from graphene sheets. Science 315(5811):490–493. doi:10.1126/science.1136836

Bunch JS, Verbridge SS, Alden JS et al (2008) Impermeable atomic membranes from graphene sheets. Nano Lett 8:2458–2462. doi:10.1021/nl801457b

Campbell JD (1956) On the theory of initially tensioned circular membranes subjected to uniform pressure. J Mech Appl Math 9(1):84–93

Chen C, Rosenblatt S, Bolotin KI et al (2009) Performance of monolayer graphene nanomechanical resonators with electrical readout. Nat Nanotechnol 4(12):861–867. doi:10.1038/nnano.2009.267

Di Giovanni M (1982) Flat and corrugated diaphragm design handbook. CRC Press, New York

El-Kady MF, Strong V, Dubin S et al (2012) Laser scribing of high-performance and flexible graphene-based electrochemical capacitors. Science 335(6074):1326–1330. doi:10.1126/science.1216744

Gao W, Huang R (2011) Effect of surface roughness on adhesion of graphene membranes. J Phys D Appl Phys 44(45):452001. doi:10.1088/0022-3727/44/45/452001

Garcia-Sanchez D, Van der Zande AM, Paulo AS et al (2008) Imaging mechanical vibrations in suspended graphene sheets. Nano Lett 8(5):1399–1403. doi:10.1021/nl080201h

Geim AK (2009) Graphene: status and prospects. Science 324(5934):1530–1534. doi:10.1126/science.1158877

Géminard JC, Bernal R, Melo F (2004) Wrinkle formations in axi-symmetrically stretched membranes. Eur Phys J E 15:117–126. doi:10.1140/epje/i2004-10041-1

Gómez-Navarro C, Burghard M, Kern K (2008) Elastic properties of chemically derived single graphene sheets. Nano Lett 8(7):2045–2049. doi:10.1021/nl801384y

Hencky H (1915) Über den spannungszustand in kreisrunden platten mit verschwindender biegungssteiflgkeit. Zeitschrift fur Mathematik und Physik 63:311–317

Kim KS, Zhao Y, Jang H, Lee SY, Kim JM, Kim KS, Ahn JH, Kim P, Choi JY, Hong BH (2009) Large-scale pattern growth of graphene films for stretchable transparent electrodes. Nature 457:706. doi:10.1038/nature07719

Koenig SP, Boddeti NG, Dunn ML et al (2011) Ultrastrong adhesion of graphene membranes. Nat Nanotechnol 6(9):543–546. doi:10.1038/nnano.2011.123

Lee C, Wei X, Kysar JW et al (2008) Measurement of the elastic properties and intrinsic strength of monolayer graphene. Science 321(5887):385–388. doi:10.1126/science1157996

Lin PY (1990) The in situ measurement of mechanical properties of multilayer coatings. Dissertation, Massachusetts Institute of Technology

Lin YM, Dimitrakopoulos C, Jenkins KA et al (2010) 100-GHz transistors from wafer-scale epitaxial graphene. Science 327(5966):662. doi:10.1126/science.1184289

Ma J, Jin W, Ho H et al (2012) High-sensitivity fiber-tip pressure sensor with graphene diaphragm. Opt Lett 37(13):2493–2495. doi:10.1364/OL.37.002493

Ma J, Xuan H, Ho HL, Jin W, Yang Y, Fan S (2013) Fiber-Optic Fabry-Pérot acoustic sensor with multilayer graphene diaphragm. Photonics Technol Lett 25:932–935. doi:10.1109/LPT.2013.2256343

Smith AD, Vaziri S, Delin A et al (2012) Strain engineering in suspended graphene devices for pressure sensor applications. ultimate integration on silicon (ULIS), 13th international conference on 21–24 (2012). doi:10.1109/ULIS.2012.6193347

Vlassak JJ (1994) New experimental techniques and analysis methods for the study of the mechanical properties of materials in small volumes. Dissertation, Stanford University

Yoon T, Shin WC, Kim TY et al (2012) Direct measurement of adhesion energy of monolayer graphene as-grown on copper and its application to renewable transfer process. Nano Lett 12(3):1448–1452. doi:10.1021/nl204123h